

Thermal Conductivity, Thermopower, and Figure of Merit of $\text{La}_{1-x}\text{Sr}_x\text{CoO}_3$

K. Berggold, M. Kriener, C. Zobel, A. Reichl, M. Reuther, R. Müller, A. Freimuth, and T. Lorenz
II. Physikalisches Institut, Universität zu Köln, Zùlpicher Str. 77, 50937 Köln, Germany

(Dated: October 26, 2018)

We present a study of the thermal conductivity κ and the thermopower S of single crystals of $\text{La}_{1-x}\text{Sr}_x\text{CoO}_3$ with $0 \leq x \leq 0.3$. For all Sr concentrations $\text{La}_{1-x}\text{Sr}_x\text{CoO}_3$ has rather low κ values. For the insulators ($x < 0.18$) this arises from a suppression of the phonon thermal conductivity by lattice disorder due to temperature- and/or doping-induced spin-state transitions of the Co ions. For larger x , the heat transport by phonons remains low, but an additional contribution from mobile charge carriers causes a moderate increase of κ . The thermopower of the low-doped crystals is positive and shows a pronounced maximum as a function of temperature. With increasing x , this maximum strongly broadens and its magnitude decreases. For the highest Sr content ($x = 0.3$) S becomes even negative in the intermediate temperature range. From S , κ , and the electrical resistivity ρ we derive the thermoelectric figure of merit $Z = S^2 / \kappa \rho$. For intermediate Sr concentrations we find notably large values of Z indicating that Co-based materials could be promising candidates for thermoelectric cooling.

PACS numbers: 72.15.Jf, 72.80.Ga, 71.30.+h

I. INTRODUCTION

Among transition-metal oxides cobalt compounds are of particular interest due to the possibility of the Co ions to occur in different spin states. This is a long standing issue for the almost cubic perovskite LaCoO_3 where the Co^{3+} spin state changes as a function of temperature from a non-magnetic low-spin (LS, $S=0$) state to an intermediate-spin (IS, $S=1$) or a high-spin (HS, $S=2$) state, which both are magnetic.^{1,2,3,4,5,6,7} During the last years cobaltates with layered CoO structures have also become subject of intense studies.^{8,9,10,11,12,13,14,15} It has been proposed that various of these compounds would also show temperature-dependent spin-state transitions of the Co^{3+} and/or Co^{2+} ions, but an unambiguous proof of such spin-state transitions is still missing (see e.g. Ref.15). Recently, the observation of superconductivity in $\text{Na}_x\text{CoO}_2 \cdot y\text{H}_2\text{O}$ has attracted much attention.¹⁶ The water-free parent compound Na_xCoO_2 became prominent some years ago already in a different context.¹⁷ It was found that Na_xCoO_2 with $x = 0.6$ has a metallic electrical conductivity σ , but a low thermal conductivity κ and, in addition, a large thermopower S . The combination of large σ , small κ , and large S values is a precondition for effective thermoelectric cooling. The performance of thermoelectric devices depends on the so-called thermoelectric figure of merit $Z = S^2 / \kappa \rho$ where $\rho = 1/\sigma$ denotes the electrical resistivity. For an effective cooling, ZT values (T is the absolute temperature) of order unity should be reached and are found for instance in Bi-based alloys, some thin-film devices or quantum dot superlattices.^{18,19} For comparison, typical metals have much smaller ZT values of order 10^{-4} . In this respect it was quite surprising that Na_xCoO_2 has $ZT \simeq 0.03$ for $150\text{ K} \leq T \leq 300\text{ K}$. The enhanced figure of merit of Na_xCoO_2 mainly arises from an enhanced thermopower.²⁰ Based on a study of the magnetic-field dependence $S(H)$ of Na_xCoO_2 it has been

argued that the spin entropy is the likely source for the large thermopower.²¹

A large thermopower occurs also in $\text{La}_{1-x}\text{Sr}_x\text{CoO}_3$.²² This motivated us to study the transport properties of this series in order to determine experimentally the ZT values and their dependence on temperature and doping. Another motivation for our study was that the previous results do not give a consistent picture of the transport properties. For example, from various anomalous features in the temperature dependencies of S , ρ , and the magnetic susceptibility χ a complex phase diagram was proposed for the $\text{La}_{1-x}\text{Sr}_x\text{CoO}_3$ system.²² It has, however, been argued that the occurrence of some of these anomalous features depends on the preparation technique of the polycrystals.²³ In fact, the phase diagram derived from $\rho(T)$ and $\chi(T)$ measured on $\text{La}_{1-x}\text{Sr}_x\text{CoO}_3$ single crystals^{24,25} is much less complex than the previous one²². Moreover, the temperature dependencies of S for undoped LaCoO_3 reported in Refs.3 and 26 are contradictory. For $T > 400\text{ K}$ both reports find a positive thermopower of order $+50\text{ }\mu\text{V/K}$, which slightly increases with decreasing temperature. For $T < 400\text{ K}$, however, a further increase of S with a maximum of about $+1200\text{ }\mu\text{V/K}$ around 100 K is found in Ref.3, whereas a sign change of S and a decrease to about $-400\text{ }\mu\text{V/K}$ for $T \simeq 200\text{ K}$ is reported in Ref.26. The thermal conductivity of the $\text{La}_{1-x}\text{Sr}_x\text{CoO}_3$ system has to our knowledge not yet been studied at all.

In this report we present an experimental study of the thermal conductivity and the thermopower of a series of single crystals of $\text{La}_{1-x}\text{Sr}_x\text{CoO}_3$ with $0 \leq x \leq 0.3$. The paper is organized as follows: In the next section we briefly describe the experimental setup and introduce the crystals, which (partly) have already been used in previous studies.^{7,25,27,28} In section III our measurements of κ and S are discussed and we derive the thermoelectric figure of merit for the $\text{La}_{1-x}\text{Sr}_x\text{CoO}_3$ series. The main results are summarized in the last section.

II. EXPERIMENTAL

The single crystals used in this study have been grown by a floating-zone technique in an image furnace. Details of the sample preparation and their characterization by X-ray diffraction, magnetization, and resistivity measurements are given in Ref. 25. At low temperatures LaCoO_3 is a good insulator, but with increasing Sr content the resistivity systematically decreases and $\text{La}_{1-x}\text{Sr}_x\text{CoO}_3$ becomes metallic for $x > 0.18$. Samples with Sr concentrations above the metal insulator transition show ferromagnetic order with transition temperatures T_c around 220 K, which slightly increase with x . The magnetic order is accompanied by a kink-like decrease of $\rho(T)$ below T_c .²⁵

The nominal valence of the Co ions does not only depend on the Sr content, but also on the oxygen concentration, i.e. the amount n of charge carriers in $\text{La}_{1-x}\text{Sr}_x\text{CoO}_{3+\delta}$ is given by $n = x + 2\delta$. Positive (negative) values of n mean hole (electron) doping and formally an amount n of the Co^{3+} ions is transformed into Co^{4+} (Co^{2+}).^{29,30} Because of the high oxidation state of Co^{4+} , one may suspect that with increasing Sr concentration the amount of oxygen vacancies also increases, i.e. an increasing x could be partially compensated by a decreasing δ . In order to check this we have determined the oxygen content of the entire series $\text{La}_{1-x}\text{Sr}_x\text{CoO}_{3+\delta}$ by thermogravimetric analysis (TGA/SDTA851, Mettler-Toledo). Pieces of about 50 mg of the single crystals have been ground and heated up to 900°C in a reducing atmosphere (N_2 with 5% H_2) in order to decompose $\text{La}_{1-x}\text{Sr}_x\text{CoO}_{3+\delta}$ into La_2O_3 , SrO and elementary Co.^{31,32,33} The value of δ is then calculated from the measured weight loss. We have tested the reproducibility of our method by repeatedly measuring amounts of about 50 mg from the same badge of a LaCoO_3 polycrystal. The different results agree to each other within ± 0.01 , which is comparable to the uncertainty of the same and alternative methods of oxygen-content determination in cobaltates.^{31,32,33} A scatter of ± 0.01 is also present in the determined oxygen contents of our $\text{La}_{1-x}\text{Sr}_x\text{CoO}_{3+\delta}$ crystals. A linear fit of $\delta(x)$ yields a weak decrease $d\delta/dx = -0.05$. Therefore we determine the charge carrier content via $n(x) = x - 0.1 \cdot x$, i.e. our analysis reveals a 10% reduction of the charge-carrier content with respect to the Sr content. We do not calculate $n = x + 2\delta$ for each crystal individually, because the scatter of δ would correspond to a scatter of the charge carrier content of ± 0.02 , which can be excluded for the studied crystals from the measurements of the magnetization and resistivity (see Ref. 25). Both quantities vary monotonously as a function of x for $0 \leq x \leq 0.3$. Thus the scatter of n between samples with neighboring x is much smaller than their difference Δx , which amounts e.g. to only 0.01 for the lowest concentrations. This conclusion is also confirmed by the data presented in this report. The only exception is the thermopower of nominally undoped LaCoO_3 , which will be discussed below.

The measurements of thermal conductivity and thermopower have been performed by a steady-state technique. One end of the rectangular bar-shaped crystals of typical dimensions $1 \times 2 \times 4 \text{ mm}^3$ has been glued on a temperature-stabilized Cu plate using an insulating varnish (VGE-7031, LakeShore). A small resistor has been attached to the other end of the sample in order to produce a heat current through the sample. The corresponding temperature gradient over the sample was measured by a differential Chromel-Au+0.07%Fe or a Chromel-Constantan thermocouple which has also been glued to the sample. Typical temperature gradients were of the order of 0.2 K. In addition, two gold contacts have been evaporated on the sample surface and two copper leads have been connected to these contacts by conductive silver epoxy in order to determine the thermopower. All offset voltages and the thermopower of the Copper leads have been carefully subtracted. With our setup we do not obtain reliable results for S on insulating samples with resistivities of the order of $10^9 \Omega\text{cm}$ or larger, as it is the case for $\text{La}_{1-x}\text{Sr}_x\text{CoO}_3$ with $x \leq 0.002$ below about 100 K. The absolute accuracy of the thermal conductivity and thermopower measurements is restricted to about 10% by uncertainties in the sample geometry, whereas the relative accuracy is of the order of a few percent.

III. RESULTS AND DISCUSSION

A. Thermal Conductivity

In Fig. 1 we show the thermal conductivity of $\text{La}_{1-x}\text{Sr}_x\text{CoO}_3$. We concentrate first on the undoped compound. In an insulator like LaCoO_3 the heat is usually carried by acoustic phonons. Optical phonons play a minor role since their dispersion is typically much weaker than that of the acoustic branches. A qualitative understanding of the phononic heat transport is obtained from the relation $\kappa \propto cv\ell$ where c , v , and ℓ denote the specific heat, the sound velocity and the mean free path of the phonons, respectively. At low temperatures ℓ is determined by lattice imperfections, or by the sample dimensions in very clean crystals, and the temperature dependence of κ follows that of the specific heat, i.e. $\kappa \propto c \propto T^3$ for $T \rightarrow 0 \text{ K}$. At intermediate temperatures a maximum of κ occurs, when phonon-phonon Umklapp scattering becomes important and leads to a decrease of ℓ with increasing temperature. At high temperatures ℓ is proportional to the number of phonons, i.e. $\ell \propto 1/T$ and κ follows roughly a $1/T$ dependence if the temperature dependence of c is not too strong, which is the case when the Debye temperature is approached.

At first glance the results on LaCoO_3 seem to be consistent with usual phononic heat transport. However, a closer inspection of the data reveals several anomalous features. The thermal conductivity above about 100 K is anomalously small and its temperature dependence is

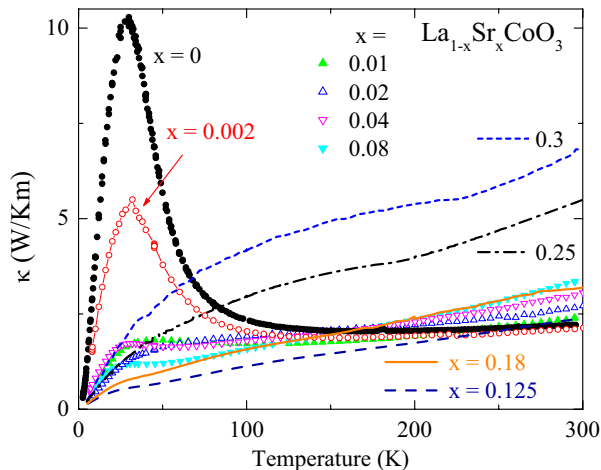


FIG. 1: Thermal conductivity of $\text{La}_{1-x}\text{Sr}_x\text{CoO}_3$ as a function of temperature for different doping x .

very unusual, since above 150 K the thermal conductivity slightly increases with increasing temperature. The small absolute values cannot be attributed to strong defect scattering, since conventional defect scattering does not vanish below 100 K so that κ would not increase and show a maximum below 100 K. Therefore, the small κ and its unusual temperature dependence indicate that an unusual, additional scattering mechanism is active above about 25 K. It is, in principle, possible that low-lying optical phonons cause resonant scattering of acoustic phonons and therefore suppress the heat current in a certain temperature range.³⁴ This could be an intrinsic feature of the phonons of the cubic perovskite structure or soft phonon modes could arise from a structural instability. However, there is, to our knowledge, no evidence for one of these scenarios. Thus we regard an anomalous damping by optical phonons as rather unlikely.

In LaCoO_3 there is another source for an unusual heat conductivity, which is related to the temperature-induced spin-state transition. With increasing temperature a thermal population of the IS (or HS) state takes place. As has been shown in Refs. 7, 27 this causes a strongly anomalous thermal expansion above about 25 K. A microscopic picture of the anomalous thermal expansion is obtained from the fact that in the LS state all six 3d electrons are in the t_{2g} orbitals, whereas in the IS or HS states also e_g orbitals are occupied. Since the e_g orbitals point towards the O^{2-} ions their population will expand the corresponding CoO_6 octahedra. Above 25 K LaCoO_3 will therefore contain smaller and larger CoO_6 octahedra with Co^{3+} ions in the LS and IS (HS) state, respectively. This implies an increasing lattice disorder above 25 K, and therefore an additional suppression of the thermal conductivity. The disorder and thus the suppression of κ is most pronounced for an equal number of LS and IS (HS) ions. For the proposed LS to IS state scenario of LaCoO_3 with an energy gap $\Delta \simeq 180$ K between the LS and IS states an equal occupation of LS

and IS ions is expected around $T \simeq 165$ K. Therefore the strong reduction of κ above 25 K, its small absolute values and the weak minimum around 150 K can arise from temperature-induced LS-IS disorder. This picture, which has also been proposed in Ref. 35, yields a consistent interpretation of the thermal conductivity data of LaCoO_3 . We note that the spin-state transition appears very favorable for the search of large ZT values, because it may intrinsically suppress κ . A more quantitative study of the influence of the spin-state transition on κ is currently underway.

The thermal conductivity of the crystal with $x = 0.002$ is similar to that of pure LaCoO_3 , but the low-temperature maximum of κ is already strongly suppressed. For higher Sr doping this maximum is almost completely absent and κ increases continuously with increasing temperature. The room temperature values of κ lie between 2 and 3 W/Km for all crystals with $x \leq 0.18$. We attribute the drastic suppression of κ at low temperatures to a Sr-induced disorder, which hinders a strong increase of ℓ for $T \rightarrow 0$ K. Probably this disorder does not solely arise from the bare difference between La^{3+} and Sr^{2+} ions. From magnetization measurements it is found that for $x \leq 0.01$ so-called magnetic polarons with high spin values ($S = 10 - 16$) are formed.³⁶ The idea is, that the divalent Sr^{2+} ions nominally cause the same amount of Co^{4+} ions, and that these magnetic ions induce a spin-state transition of the neighboring Co^{3+} ions from LS to IS or HS states. Due to such a polaron formation the disorder is strongly enhanced for the lowest Sr concentrations, whereas for larger x the polarons start to overlap and the enhancement becomes less effective.

Samples with $x > 0.18$ show metallic conductivity and ferromagnetic order at low temperatures. In this concentration range one expects that magnetic polarons become much less important. However, the low-temperature peak of κ remains absent, since the Sr concentration is so large, that the bare doping-induced lattice disorder is sufficient to suppress the low-temperature peak. Moreover, the Sr doping induces mobile charge carriers, which serve as additional scatterers for the phonons.

The mobile charge carriers for larger x are expected to transport heat, too. The total thermal conductivity therefore consists of a phononic contribution and a contribution of mobile charge carriers, i.e. $\kappa = \kappa_{ph} + \kappa_{ch}$. Usually, κ_{ch} can be estimated by the Wiedemann-Franz law, which relates κ_{ch} to the electrical conductivity according to $\kappa_{ch} \simeq L_0 \sigma T$. Here, $L_0 = 2.44 \cdot 10^{-8} \text{ V}^2/\text{K}^2$ denotes the Sommerfeld value of the Lorenz number. From the room temperature values of ρ we estimate $\kappa_{ch}(300 \text{ K}) \simeq 0.4, 0.9, 1.6$ and 2.7 W/Km for $x = 0.125, 0.18, 0.25$ and 0.3 , respectively, and $\kappa_{ch} \ll \kappa$ for smaller x . Additional heat conduction by charge carriers is therefore relevant for metallic $\text{La}_{1-x}\text{Sr}_x\text{CoO}_3$ only and explains why the crystals with $x \geq 0.25$ have significantly larger $\kappa(T)$ values for $T > 100$ K than the insulating samples with $x < 0.18$.

For $x = 0.25$ and 0.3 anomalies of κ occur around

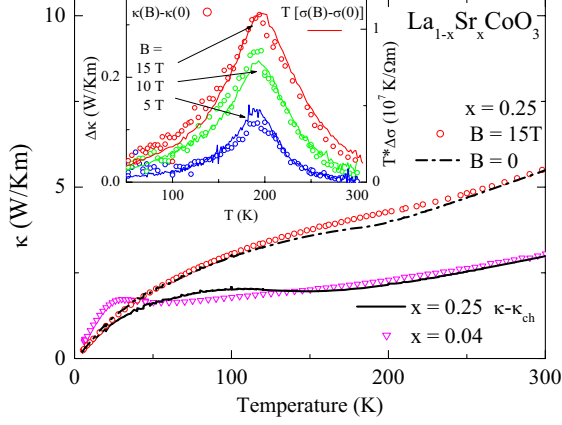


FIG. 2: Thermal conductivity κ of $\text{La}_{1-x}\text{Sr}_x\text{CoO}_3$ with $x = 0.25$ as a function of temperature measured in 15 T (\circ) and in zero magnetic field ($-\cdot-$). The solid line is the phononic contribution κ_{ph} of the $x = 0.25$ crystal, which is obtained by $\kappa_{ph} = \kappa(B) - LT\sigma(B)$ using the electrical conductivity σ and the Lorenz number L . For comparison κ of the $x = 0.04$ sample (∇) is also depicted. The Inset shows the magnetic-field dependencies $\Delta\kappa(B) = \kappa(B) - \kappa(B = 0)$ (\circ , left y scale) and $T\Delta\sigma(B) = T[\sigma(B) - \sigma(B = 0)]$ ($—$, right y scale) for $B = 5, 10$, and 15 T, respectively. The value of the Lorenz number is obtained from the field- and temperature-independent scaling factor between both quantities, i.e. via $L = \Delta\kappa(B) / [T\Delta\sigma(B)] = 2.9 \cdot 10^{-8} \text{ V}^2/\text{K}^2$.

200 K and 230 K, respectively, i.e. close to the respective ferromagnetic ordering temperatures T_c . Below T_c , κ increases and we attribute this to the decrease of ρ below T_c ,²⁵ which leads to a corresponding increase of κ_{ch} . Since the charge transport close to T_c depends on a magnetic field in $\text{La}_{1-x}\text{Sr}_x\text{CoO}_3$,³⁷ we may analyze κ_{ch} for $x = 0.25$ in more detail by comparing the magnetic-field dependencies of κ and $\sigma = 1/\rho$ (Fig. 2). We find an increase of κ with increasing field, that is most pronounced around 200 K where the strongest magnetic-field induced suppression of ρ is observed, too.³⁷ Under the reasonable assumption of a negligible field dependence of κ_{ph} we obtain $\Delta\kappa(T, B) = \kappa(T, B) - \kappa(T, 0) = \kappa_{ch}(T, B) - \kappa_{ch}(T, 0)$, and the Lorenz number is given by the relation $L = \Delta\kappa(T, B) / T\Delta\sigma(T, B)$ with $\Delta\sigma(T, B) = \sigma(T, B) - \sigma(T, 0)$. As shown in the inset of Fig. 2 the scaling relation between $\Delta\kappa$ and $T\Delta\sigma(T, B)$ is well fulfilled over the entire temperature and magnetic-field range studied here. From this scaling we find $L = 2.9 \cdot 10^{-8} \text{ V}^2/\text{K}^2$, which is about 20% larger than L_0 . The phononic thermal conductivity for $x = 0.25$ is then obtained by $\kappa_{ph} = \kappa(B) - LT\sigma(B)$ and found to agree well with those of the low-doped samples.

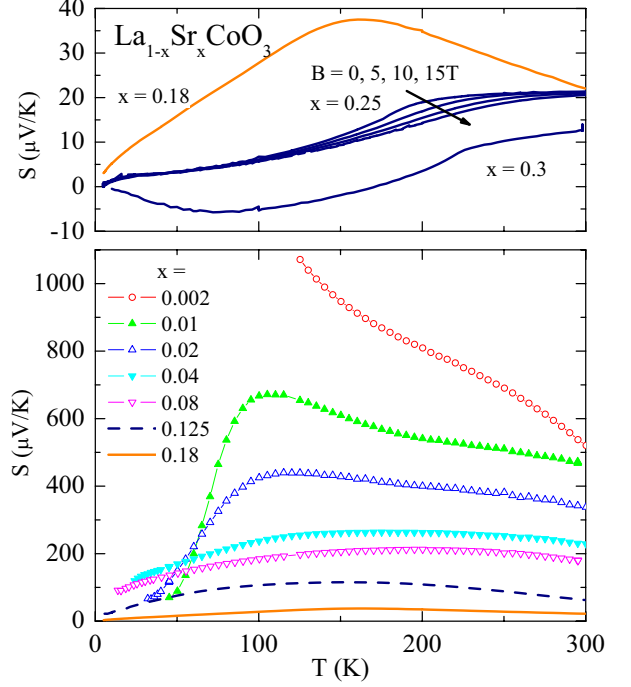


FIG. 3: Thermopower S of $\text{La}_{1-x}\text{Sr}_x\text{CoO}_3$ as a function of temperature for different doping $x > 0$. For $x = 0.25$ we show $S(T)$ also for different magnetic fields.

B. Thermopower

The thermopower measurements of the $\text{La}_{1-x}\text{Sr}_x\text{CoO}_3$ series for $x > 0$ are presented in Fig. 3. For the crystal with the lowest Sr content $x = 0.002$ we find a large positive thermopower which increases with decreasing temperature. As mentioned above we could not determine S for highly insulating crystals with $\rho \gtrsim 10^9 \Omega\text{cm}$ as it is the case for this crystal below about 100 K. With increasing Sr content S systematically decreases and for $0.01 \leq x \leq 0.18$ all $S(T)$ curves show maxima which become less pronounced and slightly shift towards higher temperature. We note that additional anomalies observed in the temperature dependence $S(T)$ of polycrystalline $\text{La}_{1-x}\text{Sr}_x\text{CoO}_3$ (Ref. 22) are not reproduced by our single-crystal data. Such a difference has already been observed in magnetization data, and gives further evidence that these additional anomalies are not an intrinsic feature of $\text{La}_{1-x}\text{Sr}_x\text{CoO}_3$.

For the metallic samples with $x \geq 0.25$ $S(T)$ varies only weakly with temperature between 300 K and T_c . Around T_c a sharp kink occurs and S strongly decreases. For $x = 0.3$ there is even a sign change and S becomes negative for $T < 170$ K. The sensitivity of S to the magnetic ordering indicates that a considerable contribution of S arises from magnetic entropy. Therefore, one may also expect a pronounced magnetic-field dependence $S(B)$ as has been pointed out recently.²¹ As shown in Fig. 3 we find indeed a strong magnetic-field induced

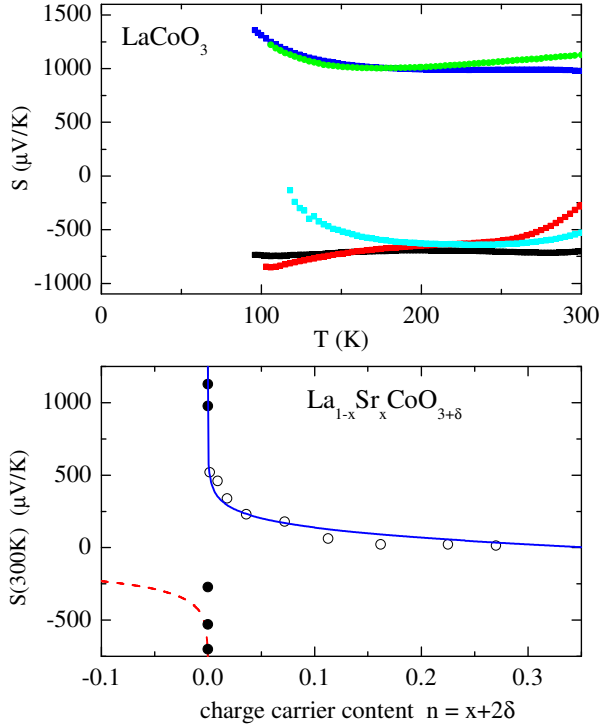


FIG. 4: Top: Thermopower S as a function of temperature for 5 different crystals of nominally undoped LaCoO_3 . Bottom: Room-temperature values $S(300\text{ K})$ as a function of the charge carrier concentration $n = x + 2\delta$ for Sr-doped (\circ) and pure (\bullet) LaCoO_3 . The lines are calculated via Eq. 1. (see text.)

suppression of S , that is most pronounced around T_c . This arises from the fact that the magnetic entropy may be strongly reduced by available magnetic-field strengths only around T_c . For higher temperatures thermal disorder becomes too large ($k_B T \gg g\mu_B B$) and for $T \ll T_c$ the magnetic entropy is already frozen by the magnetic exchange coupling.

At high enough temperatures the thermopower is expected to be determined by the so-called Heikes formula (see e. g. Ref. 38). This general expression has been refined for the case of doped cobaltates in Ref. 39 to

$$S = -\frac{k_B}{e} \left[\ln \left(\frac{n}{1-n} \right) + \ln \left(\frac{g_3}{g_4} \right) \right]. \quad (1)$$

Here, n denotes the content of Co^{4+} ions and g_3 (g_4) is the number of possible configurations of the Co^{3+} (Co^{4+}) ions, which is, in general, given by the product of orbital and spin degeneracy. If different spin states of the $\text{Co}^{3+/4+}$ ions are close enough in energy, the number of possible configurations may further increase.³⁹

In the lower panel of Fig. 4 we show the room-temperature values of S for $\text{La}_{1-x}\text{Sr}_x\text{CoO}_3$ (open symbols, $x > 0$) as a function of the charge carrier content $n = 0.9 \cdot x$ as determined by thermogravimetric analysis (see above). A fit of the experimental data via Eq. 1 with the ratio g_3/g_4 as the only fit parameter yields

$g_3/g_4 \simeq 1.8$. The saturation magnetization of the samples showing ferromagnetic order ($x > 0.18$) is best described by assuming an $S = 1/2$ low-spin state for Co^{4+} and an $S = 1$ intermediate-spin state for Co^{3+} .²⁵ For this combination of spin states a ratio $g_3/g_4 = 3/2$ is expected, which is independent from the possible orbital degeneracies $\nu = 1$ or 3 as long as both, the Co^{4+} LS and Co^{3+} IS state have the same ν . If one assumes that the energy of the Co^{3+} LS state is close to that of the Co^{3+} IS state, the ratio increases to $g_3/g_4 = 2$ and $5/3$ for $\nu = 1$ and 3 , respectively. For all of these cases the experimental data are reasonably well described by Eq. 1. However, this does not exclude other spin-state combinations, since Eq. 1 is derived for the high-temperature limit, whereas in Fig. 4 the room-temperature values of S are considered and at least for the samples with $x < 0.25$ the $S(T)$ curves have a more or less pronounced negative slope at 300 K . Thus, it is possible that for higher temperatures a larger g_3/g_4 ratio would be obtained in the fit. In addition, there are also other combinations of spin states yielding g_3/g_4 ratios close to 1.8 , but these are not supported by the measured saturation magnetization. Despite these uncertainties we interpret the doping dependence of $S(300\text{ K})$ as further evidence for the $\text{Co}_{LS}^{4+}/\text{Co}_{IS}^{3+}$ combination suggested from the magnetization and resistivity data.²⁵

According to Eq. 1 the thermopower is expected to diverge for a vanishing hole content, i. e., when the nominally undoped LaCoO_3 is approached. For electron doping one may still apply Eq. 1, but with a positive sign and g_4 for the degeneracy of Co^{2+} . The dashed line in Fig. 4 is calculated for $g_4 = 4$ as expected for Co^{2+} in a HS state.³⁰ A large negative thermopower has been observed recently in electron-doped $\text{La}_{1-x}\text{Ce}_x\text{CoO}_3$.⁴⁰ For nominally undoped LaCoO_3 , we find a different sign of S for different crystals. This is shown in the upper panel of Fig. 4. Although these crystals have been grown under the same conditions, either a large negative or a large positive thermopower can be obtained. We suspect that this extreme sensitivity of S results from weak deviations in the oxygen content of $\text{LaCoO}_{3+\delta}$, which cause small concentrations 2δ of hole or electron doping depending on the sign of δ . Already extremely small values of $|\delta| < 0.002$, which are well below the accuracy of oxygen determination in cobaltates, would be sufficient to explain the observed thermopower values with $|S| > 500\text{ }\mu\text{V/K}$ in $\text{LaCoO}_{3+\delta}$. We also suspect that there are weak inhomogeneities of the oxygen content in each sample, which can strongly influence the sign and also the temperature dependence of the measured thermopower. Most probably, this is also the reason for the contradictory results for $S(T)$ obtained in Refs. 3, 26. We mention that this extreme sensitivity $S(\delta)$ is expected only for the (almost) undoped LaCoO_3 , whereas for samples with a finite Sr content the drastic influence of such small variations of δ rapidly decreases with increasing x .

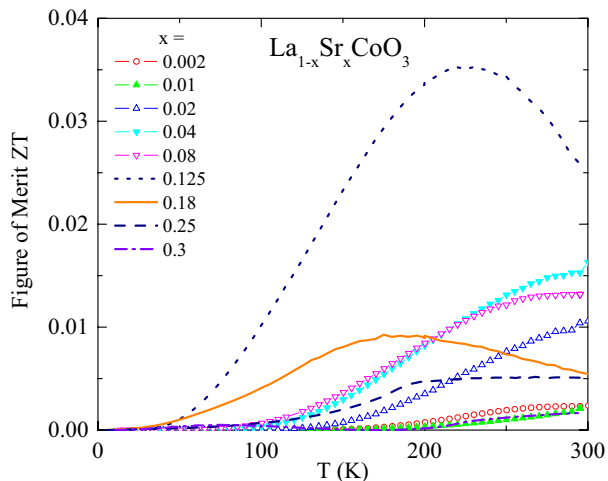


FIG. 5: Figure of merit of $\text{La}_{1-x}\text{Sr}_x\text{CoO}_3$ as a function of temperature for different doping x .

C. Figure of Merit

In Fig. 5 we present the thermoelectric figure of merit of $\text{La}_{1-x}\text{Sr}_x\text{CoO}_3$. Since the thermal conductivity for all x is rather low, one precondition for large ZT values is already fulfilled for the entire $\text{La}_{1-x}\text{Sr}_x\text{CoO}_3$ series. The very low-doped samples show in addition very large thermopower values, but their resistivities are also large and thus prevent large ZT values. Small resistivities are obtained for large x , but these samples also have smaller thermopower values. Thus the optimum figure of merit is obtained in the intermediate doping range. We find a maximum $ZT \simeq 0.035$ around 225 K, which is as large as the value observed in Na_xCoO_2 .¹⁷ These values are among the largest observed in transition metal oxides so far, but are still too small for technical applications. Nevertheless, it suggests that cobaltates may be promising candidates for thermoelectric materials, if further enhancement of ZT is possible. The fact that Co can occur in different spin states of strongly different sizes could be used to increase structural and magnetic disorder in order to suppress the thermal conductivity on the one hand and enhance the thermopower on the other.

IV. SUMMARY

We have presented a systematic study of the thermal conductivity and the thermopower of a series of single crystals of $\text{La}_{1-x}\text{Sr}_x\text{CoO}_{3+\delta}$. The thermal conductivity

is strongly suppressed for the entire doping range. In pure LaCoO_3 this suppression most probably arises from local lattice distortions due to a temperature-induced spin-state transition of the Co^{3+} ions. For small finite x , a spin-state transition of the Co^{3+} ions may be induced by the neighboring magnetic Co^{4+} ions, and so-called high-spin polarons can be formed, which also cause lattice disorder. For larger x this effect becomes less important, but scattering of phonons by mobile charge carriers will also play a role for the suppression of the thermal conductivity. For finite doping we find a large, positive thermopower, which strongly depends on temperature and doping. The room temperature values of the thermopower follow a doping dependence that is expected from a modified Heikes formula,³⁹ if we assume an intermediate-spin state for Co^{3+} and a low-spin state for Co^{4+} as it is suggested from magnetization and resistivity data.²⁵ In nominally undoped LaCoO_3 we find for different crystals either a large positive or a large negative thermopower. We suspect that this is a consequence of weak deviations ($|\delta| < 0.002$) from the nominal oxygen content causing small amounts of hole or electron doping. Most probably, a weak oxygen off-stoichiometry is also the reason for the contradictory results of the thermopower reported for LaCoO_3 previously.^{3,26} For the crystal with $x = 0.25$ both, the thermal conductivity and the thermopower show a significant magnetic-field dependence in the temperature range around the ferromagnetic ordering temperature. The field dependence of the thermal conductivity can be traced back to a field-dependent charge carrier contribution to the heat current, and the field dependence of the thermopower indicates that it contains a sizeable contribution arising from magnetic entropy. From the resistivity ρ , the thermopower S and the thermal conductivity κ we have also determined the thermoelectric figure of merit $Z = S^2 / \kappa \rho$, which strongly depends on both, doping and temperature. A maximum of $ZT \simeq 0.035$ is obtained for $x = 0.125$ and $200 \text{ K} \leq T \leq 250 \text{ K}$. This value is large, but yet too small for technical applications. Nevertheless, it indicates that Co-based materials could be interesting candidates for thermoelectric cooling.

Acknowledgments

We thank S. Heijligen for technical assistance during the measurements of the thermogravimetric analysis. We acknowledge financial support by the Deutsche Forschungsgemeinschaft through SFB 608.

¹ G. H. Jonker and J. H. Van Santen. *Physica* **XIX**, 120 (1953).

² K. Asai, O. Yokokura, N. Nishimori, H. Chou, J.M. Tranquada, G. Shirane, S. Higuchi, Y. Okajima, and K. Kohn.

Phys. Rev. B **50**, 3025 (1994).

³ M. A. Se  ar  s Rodr  guez and J. B. Goodenough. *J. of Solid State Chem.* **116**, 224 (1995).

⁴ M. A. Korotin, S. Y. Ezhov, I. V. Solovyev, V. I. Anisimov,

- D. I. Khomskii, and G. A. Sawatzky. Phys. Rev. B **54**, 5309 (1996).
- ⁵ S. Yamaguchi, Y. Okimoto, and Y. Tokura. Phys. Rev. B **55**, 8666 (1997).
 - ⁶ K. Asai, A. Yoneda, O. Yokokura, J.M. Tranquada, G. Shirane, and K. Kohn. J. Phys. Soc. Japan **67**, 290 (1998).
 - ⁷ C. Zobel, M. Kriener, D. Bruns, J. Baier, M. Grüninger, T. Lorenz, P. Reutler, and A. Revcolevschi. Phys. Rev. B **66**, 020402 (2002).
 - ⁸ T. Vogt, P.M. Woodward, P. Karen, B.A. Hunter, P. Henning, and A.R. Moodenbaugh. Phys. Rev. Lett. **84**, 2969 (2000).
 - ⁹ E. Suard, F. Fauth, V. Caignaert, I. Mirebeau, and G. Baldinozzi. Phys. Rev. B **61**, 11871 (2000).
 - ¹⁰ Y. Moritomo, T. Akimoto, M. Takeo, A. Machida, E. Nishibori, M. Takata, M. Sakata, K. Ohoyama, and A. Nakamura. Phys. Rev. B **61**, R13325 (2000).
 - ¹¹ M. Respaud, C. Frontera, J.L. García-Muñoz, M.A.G. Aranda, B. Raquet, J.M. Broto, H. Rakoto, M. Goiran, A. Llobet, and J. Rodríguez-Carvajal. Phys. Rev. B **64**, 214401 (2001).
 - ¹² H. Wu. Phys. Rev. B **64**, 92413 (2001).
 - ¹³ J. Wang, Weiye Zhang, and D. Y. Xing. Phys. Rev. B **64**, 64418 (2001).
 - ¹⁴ S. Roy, M. Khan, Y.Q. Guo, J. Craig, and N. Ali. Phys. Rev. B **65**, 64437 (2002).
 - ¹⁵ Z. Hu, H. Wu, M. W. Haverkort, H. H. Hsieh, H.-J. Lin, T. Lorenz, J. Baier, A. Reichl, I. Bonn, C. Felser, A. Tanaka, C. T. Chen, and L. H. Tjeng. Phys. Rev. Lett. **92**, 207402 (2004).
 - ¹⁶ K. Takada, H. Sakurai, E. Takayama-Muromachi, F. Izumi, R.A. Dilanian, and T. Sasaki. Nature **422**, 53 (2003).
 - ¹⁷ K. Takahata, Y. Iguchi, D. Tanaka, T. Itoh, and I. Terasaki. Phys. Rev. B **61**, 12551 (2000).
 - ¹⁸ R. Venkatasubramanian, E. Siivola, T. Colpitts, and B. O'Quinn. Nature **413**, 597 (2001).
 - ¹⁹ T.C. Harman, P.J. Taylor, M.P. Walsh, and B.E. LaForge. Science **297**, 2229 (2002).
 - ²⁰ I. Terasaki, Y. Sasago, and K. Uchinokura. Phys. Rev. B **56**, R12685 (1997).
 - ²¹ Y. Wang, N.S. Rogado, R.J. Cava, and N.P. Ong. Nature **423**, 425 (2003).
 - ²² M.A. Seánarís Rodríguez and J.B. Goodenough. J. of Solid State Chem. **118**, 323 (1995).
 - ²³ P.S. Anil Kumar, P.A. Joy, and S.K. Date. J. Appl. Phys. **83**, 7375 (1998).
 - ²⁴ M. Itoh, I. Natori, S. Kubota, and K. Motoya. J. Phys. Soc. Japan **63**, 1486 (1994).
 - ²⁵ M. Kriener, C. Zobel, A. Reichl, J. Baier, M. Cwik, K. Berggold, H. Kierspel, O. Zabara, A. Freimuth, and T. Lorenz. Phys. Rev. B **69**, 094417 (2004).
 - ²⁶ S.R. Sehlin, H.U. Anderson, and D.M. Sparlin. Phys. Rev. B **52**, 11681 (1995).
 - ²⁷ J. Baier, S. Jodlauk, M. Kriener, A. Reichl, C. Zobel, H. Kierspel, A. Freimuth, and T. Lorenz. Phys. Rev. B **71**, 014443 (2005).
 - ²⁸ R. Lengsdorf, M. Ait-Tahar, S.S. Saxena, M. Ellerby, D.I. Khomskii, H. Micklitz, T. Lorenz, and M.M. Abd-Elmeguid. Phys. Rev. B **69**, 140403(R) (2004).
 - ²⁹ In the case of hole doping this formal description must not be taken literally, because due to the high oxidation state Co^{4+} the holes are likely to enter the oxygen $2p$ states.
 - ³⁰ Note that depending on the spin states of the various Co ions hole and electron doping may be strongly different with respect to charge transport due to the so-called spin blockade effect^{40,41}.
 - ³¹ M. James, D. Cassidy, D.J. Goossens, and R.L. Withers. J. of Solid State Chem. **177**, 1886–1895 (2004).
 - ³² D.J. Goossens, K.F. Wilson, M. James, A.J. Studer, and X.L. Wang. Phys. Rev. B **69**, 134411 (2004).
 - ³³ K. Conder, E. Pomjakushina, A. Soldatov, and E. Mitberg. Mater. Res. Bull. **40**, 257–263 (2005).
 - ³⁴ Resonant scattering may also arise from scattering by magnetic excitations as it is observed in $\text{SrCu}_2(\text{BO}_3)_2$ (Ref. 42).
 - ³⁵ J.-Q. Yan, J.-S. Zhou, and J.B. Goodenough. Phys. Rev. B **69**, 134409 (2004).
 - ³⁶ S. Yamaguchi, Y. Okimoto, H. Taniguchi, and Y. Tokura. Phys. Rev. B **53**, 2926 (1996).
 - ³⁷ R. Mahendiran and A.K. Raychaudhuri. Phys. Rev. B **54**, 16044 (1996).
 - ³⁸ P.M. Chaikin and G. Beni. Phys. Rev. B **13**, 647 (1976).
 - ³⁹ W. Koshibae, K. Tsutsui, and S. Maekawa. Phys. Rev. B **62**, 6869 (2000).
 - ⁴⁰ A. Maignan, D. Flahaut, and S. Hébert. The European Phys. J. B **39**, 145–148 (2004).
 - ⁴¹ A. Maignan, V. Caignaert, B. Raveau, D. Khomskii, and G. Sawatzky. Phys. Rev. Lett. **93**, 026401 (2004).
 - ⁴² M. Hofmann, T. Lorenz, G.S. Uhrig, H. Kierspel, O. Zabara, A. Freimuth, H. Kageyama, and Y. Ueda. Phys. Rev. Lett. **87**, 047202 (2001).